Volume 5
Number 17
7 September 2024
Pages 6675–7062

Materials Advances

rsc.li/materials-advances

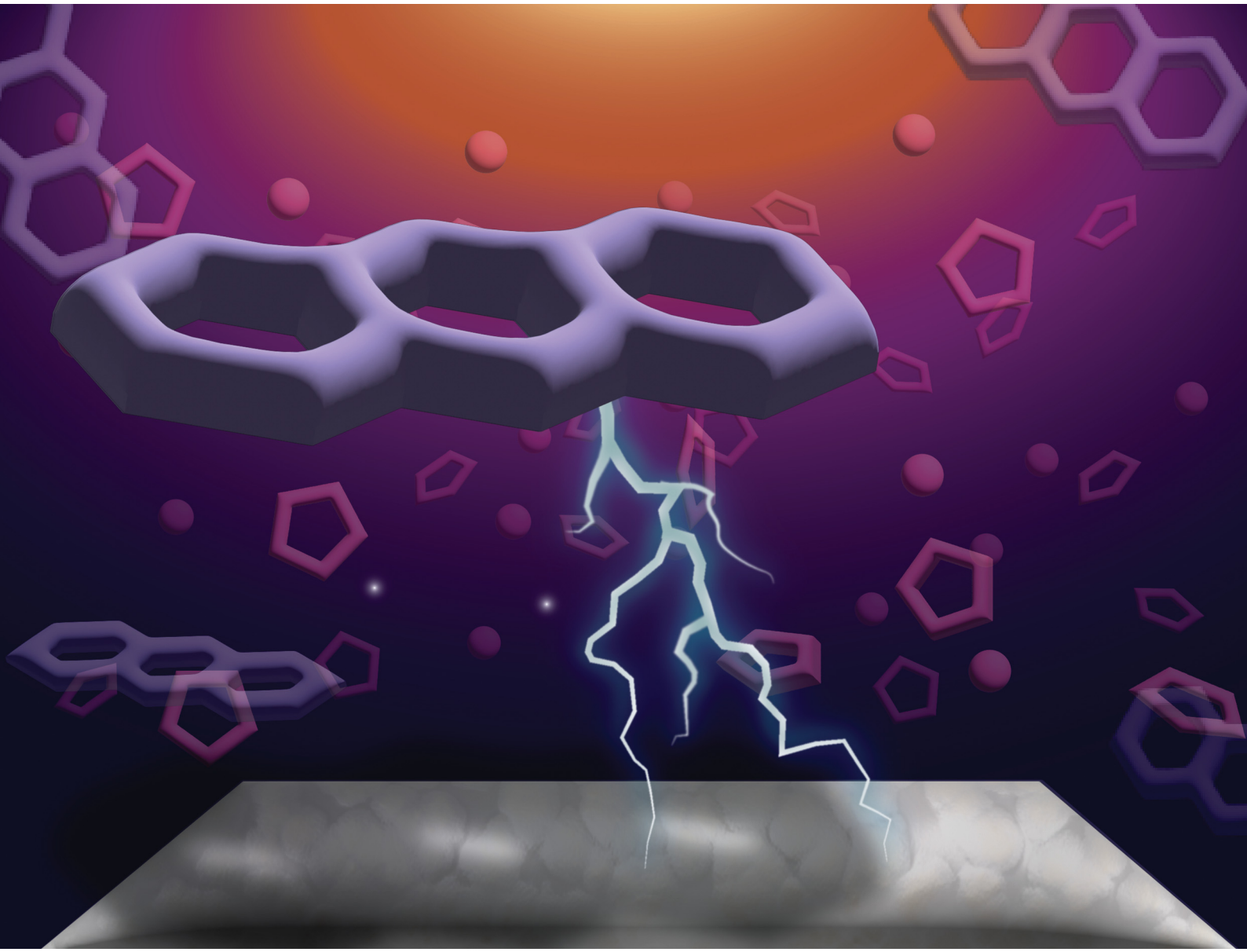

ISSN 2633-5409

ROYAL SOCIETY OF CHEMISTRY

PAPER
Ariel L. Furst *et al.*
Imidazolium-based ionic liquids support biosimilar flavin electron transfer

Materials Advances

ROYAL SOCIETY OF CHEMISTRY

PAPER

View Article Online
View Journal | View Issue

Cite this: *Mater. Adv.*, 2024, 5, 6813

Imidazolium-based ionic liquids support biosimilar flavin electron transfer†

Grace I. Anderson,[a] Alec A. Agee[a] and Ariel L. Furst *[ab]

Received 31st May 2024,
Accepted 26th July 2024

DOI: 10.1039/d4ma00558a

rsc.li/materials-advances

Understanding electron transport with electroactive microbes is key to engineering effective and scalable bio-electrochemical technologies. Much of this electron transfer occurs through small-molecule flavin mediators that perform one-electron transfers in abiotic systems but concerted two-electron transfer in biological systems, rendering abiotic systems less efficient. To boost efficiency, the principles guiding flavin electron transfer must be elucidated, necessitating a tunable system. Ionic liquids (ILs) offer such a platform due to their chemical diversity. In particular, imidazolium-containing ILs that resemble the amino acid histidine are bio-similar electrolytes that enable the study of flavin electron transfer. Using the model IL 1-ethyl-3-methylimidazolium ([Emim][BF_4]), we observe concerted two-electron transfer between flavin mononucleotide and an unmodified glassy carbon electrode surface, while a one-electron transfer occurs in standard inorganic electrolytes. This work demonstrates the power of ILs to enable the mechanistic study of biological electron transfer, providing critical guidelines for improving electrochemical technologies based on these biological properties.

Introduction

Sustainable energy technologies are essential to achieve the ambitious goals laid out by the Paris Climate Agreement. Though many such technologies have been developed, platforms that integrate biological components such as enzymes or electroactive microbes (EAMs) are increasingly popular because of their efficiency in native systems.[1,2] For example, in native enzymatic and microbial electron transfer, small-molecule, flavin-based mediators (*e.g.*, flavin mononucleotide (FMN)) are prevalent.[3–5] However, when applied to engineered technologies, electron transfer kinetics with these flavins are sluggish, limiting the utility and scalability of such systems.[6–8] Thus, engineering of the microbe-electrode interface to optimize electron transfer is key to applying EAMs in scalable energy technologies.

We recently reported that ion- and electron-conductive polymers alter the mechanism of electron transfer between FMN and carbon electrodes, enabling concerted, two-electron transfer and significantly improving the kinetics of interfacial electron transfer.[9] Additionally, the model EAM *Shewanella oneidensis* grew more robust biofilms on these materials as compared to carbon electrodes. These improvements, alongside other advancements in polymer engineering,[10] could move microbial technologies towards scalable viability. However, the need for efficient flavin-based electron transfer extends to systems far beyond *S. oneidensis*, including when direct association with the electrode is impossible. Thus, the use of a polymer-modified electrode is not ideal for many applications. Further, though we can investigate some structure–function relationships with these polymers, we are limited by synthetic challenges in generating polymer libraries with sufficient diversity.

Ionic liquids (ILs) are a class of salts composed of non-coordinating organic ions, often characterized by melting temperatures below 100 °C. ILs boast a wide range of desirable properties including low vapor pressure, good thermal and chemical stability, and, notably, wide windows of electrochemical stability.[11–13] Moreover, these salts have nearly unlimited possibilities for chemical structure and synthesis strategies, enabling their tunability for key properties.[11,14,15] These advantages, along with their improved solubilizing capability, polarity, and non-volatility, have led to the use of ILs as alternative solvents. Additionally, as liquids comprised entirely of ions with good electrochemical stability, ILs have also been applied as electrolytes to conventional energy systems including batteries, fuel cells, and redox flow batteries.[16–18]

The unique properties of ILs have also led to their biological application, as they can increase the solubility of small-molecule drugs and stabilize biomolecules.[19–22] Beyond biomedical applications, the properties of ILs make them promising

[a] *Department of Chemical Engineering, Massachusetts Institute of Technology, Cambridge, MA 02139, USA. E-mail: afurst@mit.edu*
[b] *Center for Environmental Health Sciences, Massachusetts Institute of Technology, Cambridge, MA 02139, USA*

† Electronic supplementary information (ESI) available. See DOI: https://doi.org/10.1039/d4ma00558a

matrices for bio-electrochemical systems. In fact, IL-derived materials such as carbon ionic liquid electrodes, IL-functionalized carbon nanomaterials, and ionic liquid polymers (ILPs) have been applied to bioelectrochemical systems (BES).[23,24] The incorporation of these materials into BESs is in its nascency, but preliminary reports with these materials are promising. The use of ILPs and IL–carbon nanomaterials in microbial fuel cells yields systems with greater stability and improved charge density as compared to their counterparts.[25,26] Taken together, the advantages of ILs make them an important class of materials to support both fundamental studies of and improvements to BESs.

Herein, we characterize the electron transfer of FMN in the presence of a model IL electrolyte, 1-ethyl-3-methylimidazolium tetrafluoroborate [Emim][BF_4]. In contrast to previous studies with IL-derived materials, here, we investigate the impact of ILs as freely-diffusing supporting electrolytes in aqueous solution, rather than as a modification to solid substrates. With these imidazolium-containing ILs, we observe concerted, two-electron transfer between the FMN and glassy carbon electrodes, just as what was previously observed with ion- and electron-transfer proficient polymers. The high local environment tunability with ILs enables their use to address fundamental questions in mediated biological electron transfer, and their ability to support concerted electron transfer with FMN opens the door for their broader use in BESs.

Results and discussion

1. Selection of materials and experimental design

Previously, we observed concerted, two-electron transfer between FMN and an electrode modified with an ion- and electron-conductive polymer. The improved electron transfer was attributed to the biosimilar structural features of poly{3-[6′-(*N*-methylimidazolium)hexyl]thiophene} (P3HT-Im^+), particularly the histidine-like imidazolium group. Concerted electron transfer was only observed when the ion-conducting imidazolium groups were incorporated in the polymer. Thus, we targeted this moiety to study using ILs in aqueous solutions.

The IL [Emim][BF_4] was selected as a model electrolyte because of its imidazolium moiety as well as its commercial availability and water solubility (Fig. 1). Importantly, this IL is widely used in both electrochemical and non-electrochemical applications. Due to its ubiquity and canonical status in IL studies, [Emim][BF_4] is ideal as a well-characterized material for these fundamental studies. In addition to containing the desired imidazolium functionality, we also found that [Emim][BF_4] improved FMN solubility in aqueous solution. For the studies described here, we compared this IL to a standard aqueous inorganic electrolyte system, potassium chloride (KCl).

Limited aqueous solubility of FMN has been a noted challenge in both electrochemical and biomedical applications, particularly for redox flow batteries.[27,28] This limitation hinders the application of this small molecule in most aqueous systems. The solubility challenge has been previously resolved through the addition of solubilizing agents like nicotinamide.[27] However, this can impact redox processes in abiotic systems and can interfere with biotic respiration or metabolism. Somewhat surprisingly, we found significantly increased FMN solubility in the IL as compared to in KCl.

Using UV-Visible (UV-Vis) spectrometry, the solubility limit of FMN in the IL electrolyte was found to be 55.74 mM, as compared to 35.76 mM in KCl electrolyte (Fig. S2, ESI†). Our observation that [Emim][BF_4] improves FMN solubility is consistent with prior reports of similar small molecule solubilization in ILs, hypothesized to be due to electrostatic interactions and polarity. Similar influences were theorized to be responsible for the improved electron transfer observed with the P3HT-Im^+ polymer. However, as the IL is not simply sequestered at the electrode surface, its influence on FMN electron transfer was expected to differ from the polymer. Thus, we electrochemically characterized the IL–FMN system to enable its direct comparison to the conductive polymer, with FMN in inorganic electrolyte used as a control.

Electrochemical measurements including cyclic voltammetry (CV), chronoamperometry (CA), and electrochemical impedance spectroscopy (EIS) were performed with a conventional

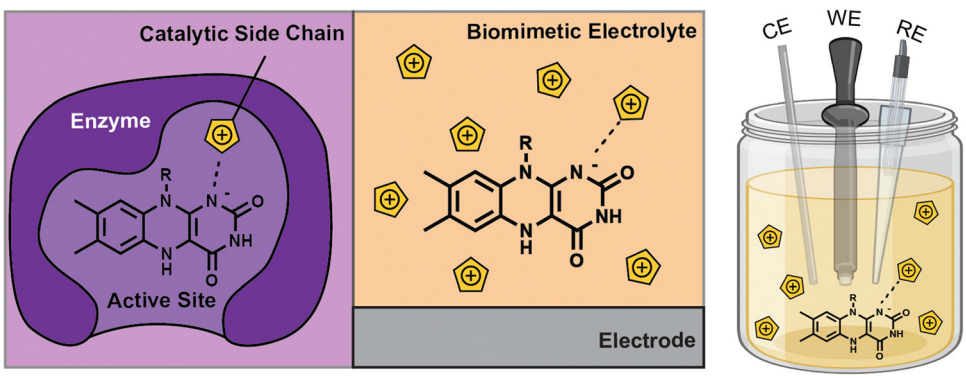

Fig. 1 Schematic representation of histidine residue facilitating electron transport of FMN in a biological microenvironment (left) compared to the imidazolium IL as a biomimetic histidine-like electrolyte to achieve similar electron transport efficiency at an electrode surface (middle). This is translated into a three-electrode electrochemical cell setup (right).

three-electrode setup using a glassy carbon (GC) working electrode, a platinum counter electrode, and an in-house generated gel-tipped Ag/AgCl reference electrode, the generation of which is described in the ESI.† [29] Our initial experiments focused on comparing FMN diffusion in the IL against KCl. We additionally evaluated the electrochemical reversibility of the FMN reduction and oxidation (redox) couple in the IL electrolyte. This information is readily determined from CV performed at varying scan rates.

2. Cyclic voltammetry

CV was initially employed to determine the reversibility of the FMN redox process. Further, upon variation of the scan rate, FMN diffusion through the IL can be evaluated. We initially determined the reversibility of FMN redox processes in our model IL using 5 mM FMN in PIPES buffer (pH 7.4) with varying concentrations of the IL electrolyte (100 mM, 300 mM, or 500 mM of [Emim][BF_4]). CV was performed over a potential window of −0.8 V to 0.0 V *vs.* Ag/AgCl, with scan rates ranging from 2 mV s^{-1} to 1 V s^{-1} (Fig. 2A). As can be seen in the CVs, the oxidative and reductive sweeps yield faradaic currents and total charges of approximately equal magnitude. Notably, at a given scan rate (200 mV s^{-1}), the IL–FMN solutions yield higher faradaic electron transfer, as indicated by larger maximum peak currents, as compared to the inorganic KCl–FMN systems (Fig. 2B and C). Even at lower electrolyte concentrations, the IL supports more efficient electron transfer than the KCl electrolyte. The peak shape and overall current resulting from CV analysis confirms that FMN maintains reversible electron transfer even at low IL electrolyte concentrations.

In addition to the peak shape of the CVs, we can use the scan rate dependence of the peak current to compare FMN diffusion in the electrolytes. Plotting the peak current against the square root of the scan rate resulted in linear traces that could be fit to the Randles–Sevcik equation (eqn (1)).

$$i = 0.4463nFAC\left(\frac{nFD}{RT}\right)^{1/2} v^{1/2} \quad (1)$$

where i (A) is the peak current, v (V s^{-1}) is the scan rate, n is the number of electrons transferred, A (cm^2) is the electrode surface area, D (cm^2 s^{-1}) is the diffusion coefficient of the FMN, and C (mol cm^{-3}) is the bulk FMN concentration. The linearity of the slope supports the conclusion that FMN acts as a freely diffusing analyte in both IL and KCl systems. This further indicates that FMN adsorption to the glassy carbon surface in the presence of [Emim][BF_4] is negligible (Fig. S3, ESI†).

The shallower slopes with IL electrolytes indicate that the overall electron transfer rate in these systems is slower than with the inorganic electrolytes. This is attributed to differences in the diffusion of FMN between these systems, which is consistent with the larger molecular diameter of the IL ions compared to the inorganic electrolyte. By integrating the faradaic currents in these CV scans, we can also determine the

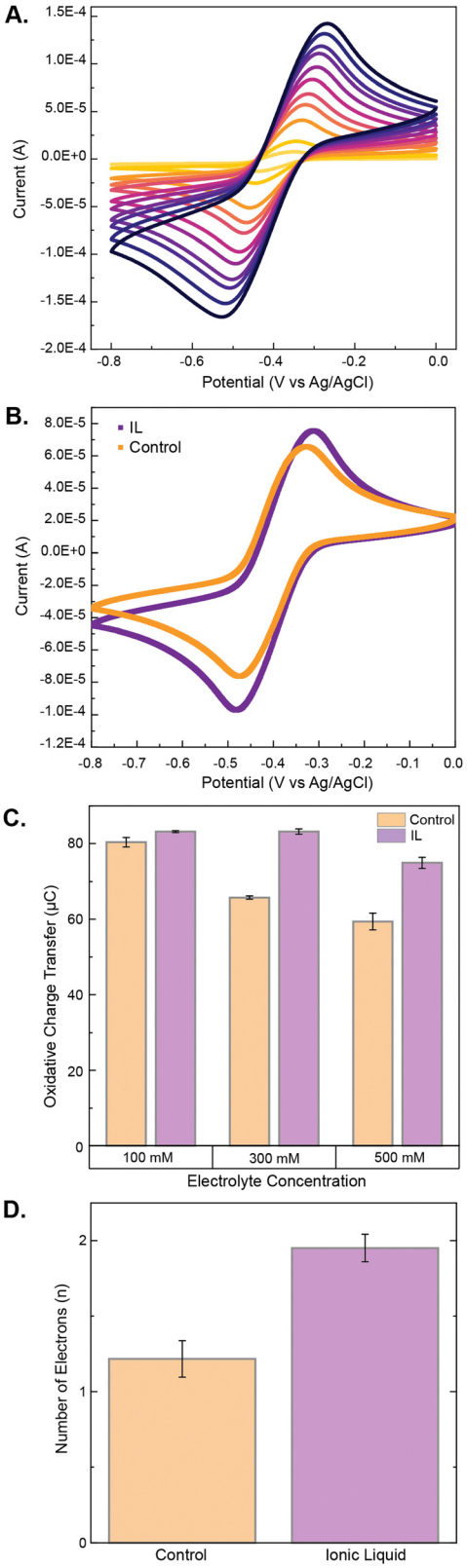

Fig. 2 Results from cyclic voltammetry analysis. (A) Array of CVs of the IL–FMN solutions at varying scan rates ranging from 2 mV s^{-1} to 1000 mV s^{-1}. (B) Comparative CVs of the IL–FMN solution (purple) and KCl–FMN solution (orange) at a 200 mV s^{-1} scan rate. (C) Oxidative charge transfer comparisons of the indicated solutions at a 200 mV s^{-1} scan rate. (D) Number of electrons transferred as calculated by combining the Randles–Sevcik and Cottrell equations. (error bars represent standard deviation for n = 3 replicates).

total charge transferred at a particular scan rate. This analysis, performed on the oxidative sweep at a 200 mV s^{-1} scan rate, revealed that total charge transfer from the FMN in the IL electrolyte was higher than in the KCl. Further, as would be expected for increasing electrolyte concentration, charge transfer increased with increasing IL concentrations (Fig. 2C).

Overall, analysis of the current generated by CV upon variation of the scan rate revealed that applying [Emim][BF_4] as a supporting electrolyte does not significantly impact the reversibility of the FMN redox couple. Further, the total charge for the IL–FMN system is higher than for KCl–FMN, indicating more efficient electron transfer than conventional, inorganic electrolytes.

3. Chronoamperometry (CA) and electron transfer

To further probe diffusion in IL electrolyte as compared to KCl, chronoamperometry at a potential of −0.7 V *vs.* Ag/AgCl was used. This potential was employed because it is significantly lower than the midpoint potential of the FMN redox couple. Thus, with this potential applied, the majority of the FMN in diffusion range of the electrode surface is reduced, generating a concentration gradient of this species. We can therefore achieve conditions that enable the study of diffusion-limited behavior and therefore the application of the Cottrell equation for analysis.

From the results of the CA combined with the CV data, we can determine the number of electrons transferred in our system. This measurement is critical, as we previously observed that concerted two-electron transfer *versus* single-electron transfer events was the key differentiator between electron-only conductive polymers and mixed-conductivity polymers to support electron transfer with FMN at *S. oneidensis* biofilms. Thus, we employed similar analysis to determine the number of electrons transferred. We graphed the CA as current measured *vs.* $1/t^{1/2}$, enabling analysis using the Cottrell equation (eqn (2) and Fig. 3A).

$$i(t) = \frac{nFAD^{1/2}C}{\pi^{1/2}} t^{-1/2} \quad (2)$$

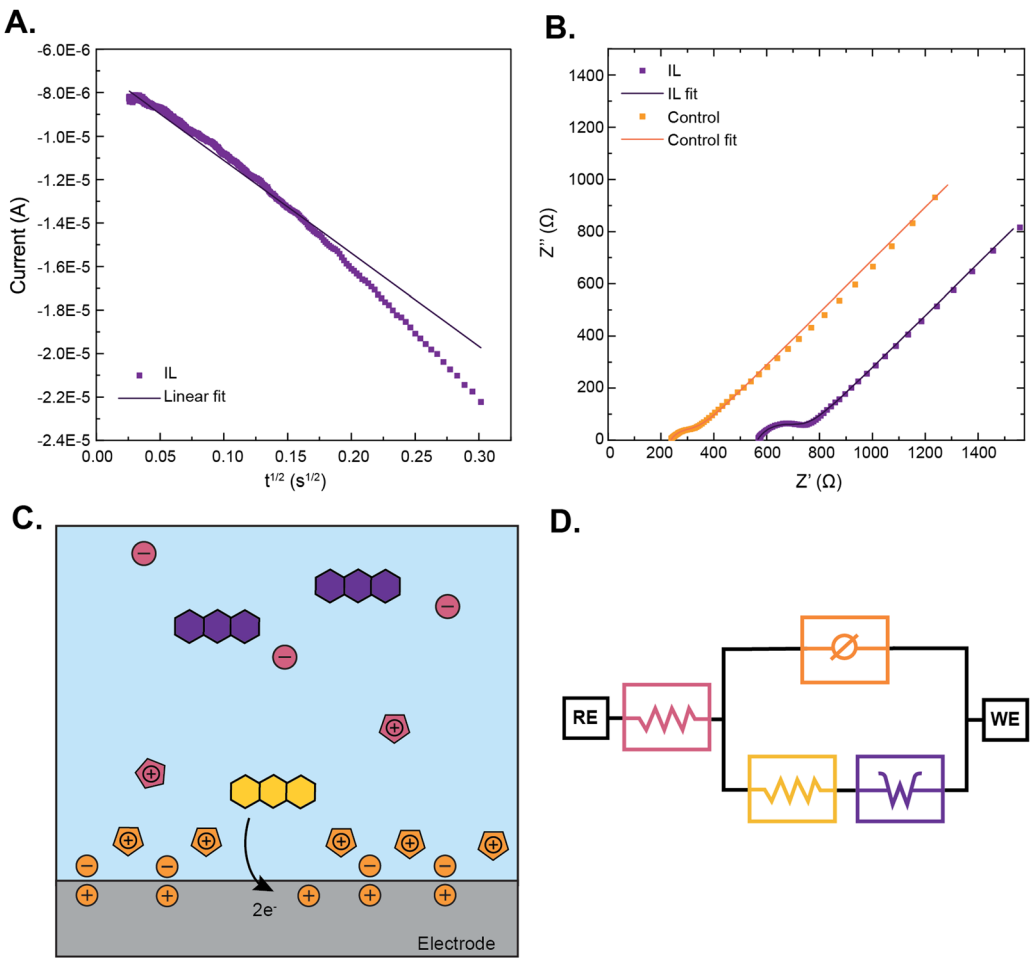

Fig. 3 (A) Linear fit of chronoamperometry data of the IL–FMN solution to the Cottrell equation. (B) Nyquist plots with circuit model fits generated from the electrochemical impedance spectra (EIS) of the IL–FMN (purple) and KCl–FMN (orange) solutions. (C) Schematic interpretation of how the imidazolium groups (pentagons) of the IL impact various electrochemical features of the circuit model, particularly the resistance and capacitance at the electric double layer. (D) The Randles equivalent cell circuit model used to fit to the EIS data with individual circuit element colors corresponding to the elements schematically displayed in (C).

where t (s) is time since the step potential was applied, i (A) is the measured current, and n, F, A, D, and C retain the same definitions as in eqn (1). Upon application of this equation to CA data, linear plots were obtained over a large time domain. Though the linear fits enabled extrapolation of parameters, we note some non-linearity at the initial and final timepoints due to inevitable non-ideality in experimental conditions. This is very common and is usually due to charging at short timescales and slight flow of the electrolyte at long time scales, as the Cottrell equation assumes completely stationary systems but electrodynamic flow is inevitable experimentally. The linear regions were selected for fitting, enabling extrapolation of a resultant line slope. That slope is equivalent to the prefactor $\frac{nFAD^{1/2}C}{\pi^{1/2}}$ of the Cottrell equation.

Upon combination of the Cottrell and Randles–Sevcik equations with numerical values extrapolated from experiments, we can solve for the number of electrons (n) transferred between FMN to the working electrode (Fig. 3B). As expected in an abiotic system, one-electron transfer was observed between FMN and the electrode in conventional KCl electrolyte (experimentally determined to be 1.22 ± 0.12).[9,30] In contrast, the calculated n value for FMN in IL electrolyte was 1.95 ± 0.09, indicating a concerted two-electron transfer process. These results suggest that [Emim][BF_4] supports two-electron transfer similarly to P3HT-Im^+ at the electrode interface. Taken together, these results further support the critical role of imidazolium groups in supporting bio-similar electron transfer.

4. Electrolyte conductivity

The simplest explanation for the difference in electron transfer observed with the IL as compared to KCl is a difference in electrolyte conductivity. Thus, we next confirmed that the conductivity of the IL is not significantly higher than the inorganic salt. Conductivities were measured in the absence of FMN for 300 mM electrolyte solutions of [Emim][BF_4] and KCl in 50 mM PIPES buffer. The IL electrolyte had a conductivity of 23.45 mS cm^{-1}, while the KCl had a conductivity of 39.02 mS cm^{-1} (Fig. S8, ESI†). Thus, the conductivity of the KCl is almost twice that of the IL, indicating that higher conductivity for the IL electrolyte is not responsible for the observed differences in electron transfer.

The lower conductivity seen in the IL electrolyte is thought to be due to the larger sizes of the ions as compared to the inorganic salt. Both the imidazolium cation and tetraborofluorate anion have distributed charge over larger molecular diameters as compared to the more compact K^+ and Cl^- ions. Additionally, ILs can form supramolecular arrangements through ion pair association and hydrogen bonding, which could further induce electrostatic screening and decrease the apparent conductivity.[31] These properties may contribute to the observed improvements in electron transfer with FMN conferred by [Emim][BF_4]. Therefore, the imidazolium ring could not only mimic histidine residues in proteins, as originally hypothesized, but could also stabilize the ion pairing in the electrolyte due to more diffuse charge distribution. The combination of these effects in the bio-similar IL electrolyte–FMN interaction could explain the efficiency in electron transfer observed. Taken together, independent of the mechanism of electron transfer, we observe increased electron transfer with our IL as compared to KCl despite its lower conductivity.

5. Impedance characterization

Because of the unexpected lack of correlation between the electrolyte conductivity and the number of electrons transferred between FMN and a substrate, we sought to better understand the general electrochemical properties and behavior of the FMN–IL system. We therefore performed electrochemical impedance spectroscopy (EIS) in the presence of 5 mM FMN in PIPES buffer with varying electrolyte conditions. Faradaic EIS was measured using the midpoint potential of the FMN as the standard potential around which the sinusoidal potential is applied. The midpoint potential was experimentally determined from CV scans by averaging the potentials of the maximum currents observed for the reductive and oxidative peaks measured at 200 mV s^{-1} with the same parameters as previously described (Fig. 3C). From these impedance measurements, Nyquist plots were generated to enable curve fitting based on a circuit model of the physical system. The Nyquist plots for both the IL and KCl demonstrate characteristics of faradaic electron transfer, with regions showing both interfacial and diffusive electron transfer. The combination of these components results in a characteristic arc at high frequencies as well as a linear region with an angle of 45° at low frequencies.[32] This linear region with such an angle is indicative of bulk electrolyte properties and represents the mass transfer of the redox-active species in the system, in this case, diffusion of FMN to the electrode surface. The elements of the impedance spectrum are consistent with the processes observed through DC electrochemical measurements (CV and CA).

Based on our understanding of the electron transfer in an IL electrolyte solution, we modeled the EIS data using a Randles cell equivalent circuit model (Fig. 3D) with a constant phase element (CPE) in place of the standard capacitance to support consistent modeling despite non-ideal capacitor behavior. The χ^2 values for both IL and inorganic electrolyte impedance spectra were low, further indicating proper fitting and validation of the physical model. Calculated circuit element values for both the IL and KCl systems can be found in Table S1 (ESI†). Perhaps the most notable differences between these two systems is evident in the comparison between the R_s and R_{ct} resistances for IL *versus* inorganic electrolyte, where R_s corresponds to the bulk solution resistance for charge carrier diffusion. The EIS fitting results indicate that the R_s values for the IL–FMN system are higher than the KCl standard, further confirming the previous observation that diffusion in the IL system is slower than with KCl electrolyte.

The other notable difference between the impedance in the two electrolytes is a larger interfacial resistance for the IL system compared to the KCl system. This difference is readily observed in the Nyquist plots, as the R_{ct} can be calculated from the diameter of the arc region at high frequencies (Fig. 3B and

Fig. S7, ESI†). R_{ct} is critical to our understanding of charge transfer at the electrode surface, as it represents the resistance of charge transfer across the electric double layer due to faradaic reaction at this surface. We attribute this to the larger cation size and asymmetry of the ionic liquid compared to the much smaller and compact K^+ cation, creating a thicker and less well-ordered electric double layer (EDL) at the electrode surface (Fig. 3C). Interestingly, this higher charge transfer resistance does not negatively impact the electron transfer occurring between FMN and the electrode surface, as demonstrated by the combined CV and CA results. This is possibly explained by the high overpotentials utilized in these experiments, overcoming kinetic limitations. Additionally, the electric double layer of imidazolium ions creates a bio-similar microenvironment that readily supports a concerted two-electron transfer for FMN.

Conclusion

Sustainable energy technologies must be implementable at scale in order to meet global carbon emissions goals. Bio-electrochemical systems enable the generation of clean energy but are limited by sluggish electron transfer. We recently reported that ion- and electron-conductive polymers support bio-similar concerted two-electron transfer between the mediator FMN and carbon electrodes. We similarly observed this boosted electron transfer with FMN to glassy carbon electrodes in the presence of the ionic liquid [Emim][BF_4]. This improved electron transfer occurs despite slower FMN diffusion and lower electrolyte conductivity as compared to conventional inorganic electrolytes. As both the polymers and ionic liquid that boost FMN electron transfer contain histidine-like imidazolium moieties, these studies support the importance of such components for scaling sustainable technologies such as microbial fuel cells. Further, probing biological electron transfer with a diverse catalog of ionic liquids may present a practical and facile approach for developing novel bio-inspired materials to improve bio-electrochemical technologies.

Data availability

The data supporting this article have been included as part of the ESI.†

Conflicts of interest

There are no conflicts to declare.

Acknowledgements

We would like to thank Dr Jonathan Cottet for support with conductivity measurements and Dr Jerome Babauta of Gamry Instruments for guidance on EIS experiments. Research reported in this publication was supported by funding from the Army Re-search Office (W911NF- 22-1-0106), the National Institutes of Health-NIEHS (Core Center Grants P42-ES027707 and P30-ES002109), and the MIT Energy Initiative (Seed Grant). G. A. and A. A. are supported by the National Science Foundation Graduate Research Fellowship Program under grants 2141064, 1745302, and 1650114.

References

1 R. Prashanthi, A Review on Microbial Fuel Cell and Green Energy, *Ionics*, 2023, **29**(5), 1667–1697, DOI: **10.1007/s11581-023-04956-6**.
2 A. J. Slate, K. A. Whitehead, D. A. C. Brownson and C. E. Banks, Microbial Fuel Cells: An Overview of Current Technology, *Renewable Sustainable Energy Rev.*, 2019, **101**, 60–81, DOI: **10.1016/j.rser.2018.09.044**.
3 S. Ikeda, Y. Takamatsu, M. Tsuchiya, K. Suga, Y. Tanaka, A. Kouzuma and K. Watanabe, *Shewanella oneidensis* MR-1 as a Bacterial Platform for Electro-Biotechnology, *Essays Biochem.*, 2021, **65**(2), 355–364, DOI: **10.1042/EBC20200178**.
4 E. D. Brutinel and J. A. Gralnick, Shuttling Happens: Soluble Flavin Mediators of Extracellular Electron Transfer in Shewanella, *Appl. Microbiol. Biotechnol.*, 2012, **93**(1), 41–48, DOI: **10.1007/s00253-011-3653-0**.
5 K. S. Aiyer, How Does Electron Transfer Occur in Microbial Fuel Cells?, *World J. Microbiol. Biotechnol.*, 2020, **36**(2), 19, DOI: **10.1007/s11274-020-2801-z**.
6 H.-S. Lee, Electrokinetic Analyses in Biofilm Anodes: Ohmic Conduction of Extracellular Electron Transfer, *Bioresour. Technol.*, 2018, **256**, 509–514, DOI: **10.1016/j.biortech.2018.02.002**.
7 Y. Li, J. Liu, X. Chen, J. Wu, N. Li, W. He and Y. Feng, Tailoring Surface Properties of Electrodes for Synchronous Enhanced Extracellular Electron Transfer and Enriched Exoelectrogens in Microbial Fuel Cells, *ACS Appl. Mater. Interfaces*, 2021, **13**(49), 58508–58521, DOI: **10.1021/acsami.1c16583**.
8 E. Zhou, Y. Lekbach, T. Gu and D. Xu, Bioenergetics and Extracellular Electron Transfer in Microbial Fuel Cells and Microbial Corrosion, *Curr. Opin. Electrochem.*, 2022, **31**, 100830, DOI: **10.1016/j.coelec.2021.100830**.
9 A. Agee, T. M. Gill, G. Pace, R. Segalman and A. Furst, Electrochemical Characterization of Biomolecular Electron Transfer at Conductive Polymer Interfaces, *J. Electrochem. Soc.*, 2023, **170**(1), 016509, DOI: **10.1149/1945-7111/acb239**.
10 Q. Zhu, J. Hu, B. Liu, S. Hu, S. Liang, K. Xiao, J. Yang and H. Hou, Recent Advances on the Development of Functional Materials in Microbial Fuel Cells: From Fundamentals to Challenges and Outlooks, *Energy Environ. Mater.*, 2022, **5**(2), 401–426, DOI: **10.1002/eem2.12173**.
11 K. Fujita, K. Murata, M. Masuda, N. Nakamura and H. Ohno, Ionic Liquids Designed for Advanced Applications in Bioelectrochemistry, *RSC Adv.*, 2012, **2**(10), 4018, DOI: **10.1039/c2ra01045c**.
12 M. Armand, F. Endres, D. R. MacFarlane, H. Ohno and B. Scrosati, Ionic-Liquid Materials for the Electrochemical Challenges of the Future, *Nat. Mater.*, 2009, **8**(8), 621–629, DOI: **10.1038/nmat2448**.

13 M. Galiński, A. Lewandowski and I. Stępniak, Ionic Liquids as Electrolytes, *Electrochim. Acta*, 2006, **51**(26), 5567–5580, DOI: 10.1016/j.electacta.2006.03.016.
14 P. Domínguez de María, "Nonsolvent" Applications of Ionic Liquids in Biotransformations and Organocatalysis, *Angew. Chem., Int. Ed.*, 2008, **47**, 6960–6968, DOI: 10.1002/anie.200703305.
15 R. Giernoth, Task-Specific Ionic Liquids, *Angew. Chem., Int. Ed.*, 2010, **49**(16), 2834–2839.
16 A. Ejigu, P. A. Greatorex-Davies and D. A. Walsh, Room Temperature Ionic Liquid Electrolytes for Redox Flow Batteries, *Electrochem. Commun.*, 2015, **54**, 55–59, DOI: 10.1016/j.elecom.2015.01.016.
17 M. H. Chakrabarti, F. S. Mjalli, I. M. AlNashef, M. A. Hashim, M. A. Hussain, L. Bahadori and C. T. J. Low, Prospects of Applying Ionic Liquids and Deep Eutectic Solvents for Renewable Energy Storage by Means of Redox Flow Batteries, *Renewable Sustainable Energy Rev.*, 2014, **30**, 254–270, DOI: 10.1016/j.rser.2013.10.004.
18 S. Indris, R. Heinzmann, M. Schulz and A. Hofmann, Ionic Liquid Based Electrolytes: Correlating Li Diffusion Coefficients and Battery Performance, *J. Electrochem. Soc.*, 2014, **161**(14), A2036–A2041, DOI: 10.1149/2.0131414jes.
19 N. Adawiyah, M. Moniruzzaman, S. Hawatulaila and M. Goto, Ionic Liquids as a Potential Tool for Drug Delivery Systems, *Med. Chem. Commun.*, 2016, **7**(10), 1881–1897, DOI: 10.1039/C6MD00358C.
20 J. L. Shamshina, P. S. Barber and R. D. Rogers, Ionic Liquids in Drug Delivery, *Expert Opin. Drug Delivery*, 2013, **10**(10), 1367–1381, DOI: 10.1517/17425247.2013.808185.
21 A. Schindl, M. L. Hagen, S. Muzammal, H. A. D. Gunasekera and A. K. Croft, Proteins in Ionic Liquids: Reactions, Applications, and Futures, *Front. Chem.*, 2019, **7**, 347, DOI: 10.3389/fchem.2019.00347.
22 S. K. Shukla and J.-P. Mikkola, Use of Ionic Liquids in Protein and DNA Chemistry, *Front. Chem.*, 2020, **8**, 598662, DOI: 10.3389/fchem.2020.598662.
23 A. Safavi, N. Maleki, H. Ershadifar and F. Tajabadi, Development of a Sensitive and Selective Riboflavin Sensor Based on Carbon Ionic Liquid Electrode, *Anal. Chim. Acta*, 2010, **674**(2), 176–181, DOI: 10.1016/j.aca.2010.06.012.
24 H. Wei, X.-S. Wu, L. Zou, G.-Y. Wen, D.-Y. Liu and Y. Qiao, Amine-Terminated Ionic Liquid Functionalized Carbon Nanotubes for Enhanced Interfacial Electron Transfer of Shewanella Putrefaciens Anode in Microbial Fuel Cells, *J. Power Sources*, 2016, **315**, 192–198, DOI: 10.1016/j.jpowsour.2016.03.033.
25 H. Wei, X.-S. Wu, L. Zou, G.-Y. Wen, D.-Y. Liu and Y. Qiao, Amine-Terminated Ionic Liquid Functionalized Carbon Nanotubes for Enhanced Interfacial Electron Transfer of Shewanella Putrefaciens Anode in Microbial Fuel Cells, *J. Power Sources*, 2016, **315**, 192–198, DOI: 10.1016/j.jpowsour.2016.03.033.
26 L. Yang, W. Deng, Y. Zhang, Y. Tan, M. Ma and Q. Xie, Boosting Current Generation in Microbial Fuel Cells by an Order of Magnitude by Coating an Ionic Liquid Polymer on Carbon Anodes, *Biosens. Bioelectron.*, 2017, **91**, 644–649, DOI: 10.1016/j.bios.2017.01.028.
27 M. P. Evstigneev, V. P. Evstigneev, A. A. H. Santiago and D. B. Davies, Effect of a Mixture of Caffeine and Nicotinamide on the Solubility of Vitamin (B2) in Aqueous Solution, *Eur. J. Pharm. Sci.*, 2006, **28**(1–2), 59–66, DOI: 10.1016/j.ejps.2005.12.010.
28 D. Hey, R. B. Jethwa, N. L. Farag, B. L. D. Rinkel, E. W. Zhao and C. P. Grey, Identifying and Preventing Degradation in Flavin Mononucleotide-Based Redox Flow Batteries via NMR and EPR Spectroscopy, *Nat. Commun.*, 2023, **14**(1), 5207, DOI: 10.1038/s41467-023-40649-4.
29 A. W. Hassel, K. Fushimi and M. Seo, An Agar-Based Silver/Silver Chloride Reference Electrode for Use in Micro-Electrochemistry, *Electrochem. Commun.*, 1999, **1**(5), 180–183, DOI: 10.1016/S1388-2481(99)00035-1.
30 S. L. J. Tan, J. M. Kan and R. D. Webster, Differences in Proton-Coupled Electron-Transfer Reactions of Flavin Mononucleotide (FMN) and Flavin Adenine Dinucleotide (FAD) between Buffered and Unbuffered Aqueous Solutions, *J. Phys. Chem. B*, 2013, **117**(44), 13755–13766, DOI: 10.1021/jp4069619.
31 O. Nordness and J. F. Brennecke, Ion Dissociation in Ionic Liquids and Ionic Liquid Solutions, *Chem. Rev.*, 2020, **120**(23), 12873–12902, DOI: 10.1021/acs.chemrev.0c00373.
32 A. Ch Lazanas and M. I. Prodromidis, Electrochemical Impedance Spectroscopy–A Tutorial, *ACS Meas. Sci. Au*, 2023, **3**(3), 162–193, DOI: 10.1021/acsmeasuresciau.2c00070.